

# Phenomenological theory of phase transitions in highly piezoelectric perovskites

I. A. Sergienko\* and Yu. M. Gufan

*Institute of Physics, Rostov State University, Rostov-on-Don, 344090, Russia*

S. Urazhdin

*Department of Physics and Astronomy, Michigan State University, East Lansing, Michigan 48824*

(Received 27 September 2001; revised manuscript received 30 November 2001; published 27 March 2002)

The recently discovered fine structure of the morphotropic phase boundaries in highly piezoelectric mixture compounds  $\text{PbZr}_{1-x}\text{Ti}_x\text{O}_3$  (PZT),  $\text{Pb}(\text{Mg}_{1/3}\text{Nb}_{2/3})_{1-x}\text{Ti}_x\text{O}_3$  (PMN-PT), and  $\text{Pb}(\text{Zn}_{1/3}\text{Nb}_{2/3})_{1-x}\text{Ti}_x\text{O}_3$  (PZN-PT) demonstrates the importance of highly nonlinear interactions in these systems. We show that an adequate Landau-type description of the ferroelectric phase transitions in these compounds is achieved by the use of a twelfth-order expansion of the Landau potential in terms of the phenomenological order parameter. Group-theoretical and catastrophe-theory methods are used in constructing the appropriate Landau potential. A complete phase diagram is calculated in phenomenological parameter space. The theory describes both PZT and PZN-PT types of phase diagrams, including the newly found monoclinic and orthorhombic phases. Anomalous large piezoelectric coefficients are predicted in the vicinity of the phase transition lines.

DOI: 10.1103/PhysRevB.65.144104

PACS number(s): 77.80.Bh, 77.84.Dy, 81.30.Dz, 77.65.Bn

## I. INTRODUCTION

For many years, perovskite-type materials have been a subject of extensive research in both experimental and theoretical physics. On one hand, different representatives of the perovskite family exhibit a host of physical phenomena, such as piezoelectricity, ferroelectricity, and superconductivity; on the other hand, perovskite structure is a relatively simple and, thus, attractive object for theoretical studies.

Even though there is a long history of studies of perovskites, they still present new surprises. Recent x-ray and neutron diffraction studies on solid solutions  $\text{PbZr}_{1-x}\text{Ti}_x\text{O}_3$  (PZT),  $\text{Pb}(\text{Mg}_{1/3}\text{Nb}_{2/3})_{1-x}\text{Ti}_x\text{O}_3$  (PMN-PT), and  $\text{Pb}(\text{Zn}_{1/3}\text{Nb}_{2/3})_{1-x}\text{Ti}_x\text{O}_3$  (PZN-PT) (Refs. 1–5) have revealed new phases in the vicinity of the morphotropic phase boundary<sup>6</sup> on the  $T$ - $x$  phase diagram of the solutions. In a narrow Ti concentration range ( $x=46$ – $52\%$ ), the low-temperature structure of PZT was found to be monoclinic  $M_A$  (crystallographic symmetry  $Cm$ ) with polarization vector  $\mathbf{P}$  directed along the  $[uvv]$ ,  $u < v$  pseudocubic direction.<sup>3</sup> A similar  $M_A$  structure has also been recently seen in PMN-PT below room temperature for  $x=35\%$ .<sup>5</sup> Another fine structure of the morphotropic phase boundary has been found in PZN-PT. For  $x=9$ – $11\%$ , the low-temperature structure is orthorhombic ( $O$ ,  $Amm2$ ) with  $\mathbf{P} \parallel [101]$ .<sup>4</sup> The rhombohedral ( $R$ ,  $R3m$ ) unpoled crystal of PZN-PT ( $x=8\%$ ) was also found to exhibit irreversible monoclinic  $M_C$  ( $Pm$ ,  $\mathbf{P} \parallel [0uv]$ ) distortion when an electric field above a certain critical value is applied along the  $[001]$  pseudocubic direction.<sup>7</sup>

Early theoretical investigations of phase transitions in perovskites were concentrated on  $\text{BaTiO}_3$ , which goes through a sequence of phases upon cooling: cubic ( $C$ ,  $Pm3m$ ), tetragonal ( $T$ ,  $P4mm$ ),  $O$ , and  $R$ . Devonshire<sup>8</sup> explains the behavior of  $\text{BaTiO}_3$  within the framework of a phenomenological Landau-type expansion up to sixth order in terms of the

ferroelectric order parameter-polarization  $\mathbf{P}$ . While successfully describing the phase diagram of  $\text{BaTiO}_3$ , the potential used in Ref. 8 lacks the high-order terms necessary to describe the low-symmetry phases. Using a geometric argument based on the Curie principle, Zheludev and Shuvalov<sup>9</sup> classified possible positions of  $\mathbf{P}$  with respect to the cubic unit cell. Due to the purely symmetric nature of this approach, it fails to distinguish between monoclinic phases  $M_A$  and  $M_B$  ( $\mathbf{P} \parallel [uvv]$ ,  $u > v$ ), because these phases have the same crystallographic symmetry  $Cm$ . The group-theoretical relationship between the geometric method and Landau approach was established in Refs. 10 and 11.

Using this approach, Gufan and Sakhnenko<sup>12</sup> found that on a two-dimensional (e.g.,  $T$ - $x$ ) phase diagram of perovskites there can be a point  $(T_0, x_0)$  where five phases  $C$ ,  $R$ ,  $O$ ,  $M_C$ , and  $T$  coexist. They calculated the phase diagram in the vicinity of this five-phase point. Only small solutions of the equations of state that are close to the five-phase point were considered, justifying expansion in powers of small parameters  $T - T_0$  and  $x - x_0$ . However, the results of this work do not apply to the recently discovered phases of the mixture compounds of Pb-based complex oxides since, in this case, the  $R$ - $O$ - $T$  and  $R$ - $M_A$ - $T$  triple points are separate from the  $C$ - $R$ - $T$  triple point. Therefore, theoretical consideration cannot be limited to small solutions of the equations of state, especially for the lowest-symmetry phases.

*Ab initio*<sup>13</sup> as well as phenomenological<sup>14</sup> calculations have been used to account for the presence of monoclinic phases on the  $T$ - $x$  phase diagrams of ferroelectric perovskites. Vanderbilt and Cohen<sup>14</sup> calculate the phase diagram in the space of phenomenological parameters within the framework of Landau-Devonshire theory. Their model is based on the eighth-order expansion of the Landau potential in terms of the polarization orientation  $\mathbf{P}/|\mathbf{P}|$ . Although monoclinic phases appear in the phase diagram of the model, it does not incorporate cubic and triclinic ( $Tri$ ,  $P1$ ) phases.

Having considered a number of successively more complicated models, a natural question arises: What is the most general phenomenological model of the phase diagram of a cubic system induced by a ferroelectric order parameter? This question can be answered by use of the concept of *integrity rational basis of invariants* (IRBI), introduced in Appendix A. The IRBI can be thought of as a basis in the space of polynomials (formed from the order parameter components), which are invariant under the transformations of the symmetry group of the system. By a group-theoretical argument, if the IRBI contains polynomials of maximal order  $n$ , then at least a  $2n$ th-order phenomenological model is necessary to describe all the possible phases induced by the order parameter.<sup>15</sup> This statement is true for the irreducible representations of groups generated by reflections, including the  $Pm3m$  symmetry of the perovskite structure. We will show that, in the case of perovskites, the Landau potential has to be expanded up to the twelfth-order terms to describe the phase diagram induced by the ferroelectric order parameter.

The results of the analysis of a simple twelfth-order model are presented in this paper. In Sec. II, we present the solutions resulting in a phase diagram containing all the phases allowed by the symmetry of the ferroelectric order

parameter. In Sec. III, we fit the  $T$ - $x$  phase diagrams of PZT and PZN-PT. In Sec. IV, we discuss the piezoelectric properties of the compounds in the vicinity of the newly found phase boundaries. The Appendixes are intended to give a group-theoretical and catastrophe-theory background for some general statements we make in the text.

## II. TWELFTH-ORDER LANDAU-TYPE MODEL

Three algebraically independent  $Pm3m$ -invariant polynomials can be formed (see Appendix A) from the polarization vector components  $(P_x, P_y, P_z)$ .

$$\begin{aligned} J_1 &= P_x^2 + P_y^2 + P_z^2, \\ J_2 &= P_x^2 P_y^2 + P_y^2 P_z^2 + P_x^2 P_z^2, \\ J_3 &= P_x^2 P_y^2 P_z^2. \end{aligned} \quad (1)$$

The ferroelectric part of the Landau potential can then be expressed in terms of algebraic combinations of  $J_1$ ,  $J_2$ , and  $J_3$ . Since polynomials of up to sixth order are present in the IRBI [Eq. (1)], the Landau potential has to be expanded up to the twelfth-order terms:

$$\begin{aligned} F &= a_1 J_1 + a_2 J_1^2 + b_1 J_2 && \text{(2nd and 4th order terms)} \\ &+ a_3 J_1^3 + d_{12} J_1 J_2 + c_1 J_3 && \text{(6th order terms)} \\ &+ a_4 J_1^4 + d_{112} J_1^2 J_2 + b_2 J_2^2 + d_{13} J_1 J_3 && \text{(8th order terms)} \\ &+ a_5 J_1^5 + d_{112} J_1^3 J_2 + d_{122} J_1 J_2^2 + d_{113} J_1^2 J_3 + d_{23} J_2 J_3 && \text{(10th order terms)} \\ &+ a_6 J_1^6 + d_{1112} J_1^4 J_2 + d_{1122} J_1^2 J_2^2 + b_3 J_2^3 + d_{1113} J_1^3 J_3 + d_{123} J_1 J_2 J_3 + c_2 J_3^2 && \text{(12th order terms)} \end{aligned} \quad (2)$$

A complete investigation of extrema of the function  $F(\mathbf{P})$  in the multidimensional parameter space is a rather tedious exercise. However, the main features of the phase diagram can be obtained from simplified models based on the potential (2) with some terms omitted. The truncated potential should satisfy at least two requirements: (i) it has to be bounded from below, and (ii) it should be structurally stable in catastrophe-theory sense.<sup>15,16</sup> The latter requirement provides that small perturbations, which can arise from the terms omitted in Eq. (2), do not drastically change the results obtained in a simplified model. In Appendix B, we briefly describe how compliance with the second requirement can be verified.

A twelfth-order model

$$F_{\text{init}} = a_1 J_1 + b_1 J_2 + c_1 J_3 + a_2 J_1^2 + b_2 J_2^2 + c_2 J_3^2 \quad (3)$$

meets both requirements when  $a_2$ ,  $b_2$ , and  $c_2$  are positive quantities, while  $a_1$ ,  $b_1$ , and  $c_1$  are parameters driving phase transitions, and can be of any sign. In spite of its simplicity, model (3) is in full agreement with the results of the group-theoretical analysis of the ferroelectric phase transitions in perovskites. It gives an account of all the phases  $C$ ,

$T$ ,  $O$ ,  $R$ ,  $M_A$ ,  $M_B$ ,  $M_C$ , and  $\text{Tri}$ , and it correctly describes the phase boundaries. For example, although the symmetry groups of the phases  $M_A$  ( $M_B$ ) and  $R$  obey a group-subgroup relation  $Cm \subset R3m$ , phase transitions  $R$ - $M_A$  and  $R$ - $M_B$  cannot be of second order.<sup>11,14</sup>

A complete phase diagram of the Landau potential (3) can be constructed in the space of phenomenological parameters  $(a_1, b_1, c_1)$ . All the characteristic features can be seen from the two-dimensional cross sections in the  $a_1 b_1$  plane, as shown in Fig. 1.

Below we show how the phase diagram of Fig. 1 was obtained, using the example of phase R. Minimizing the potential (3) with respect to  $P_x, P_y, P_z$  and then imposing the condition  $P_x = P_y = P_z = P_s / \sqrt{3}$ , we obtain the value of spontaneous polarization  $P_s$  as a solution of the equation of state

$$a_1 + \frac{2}{3}(3a_2 + b_1)P_s^2 + \frac{c_1}{9}P_s^4 + \frac{4b_2}{9}P_s^6 + \frac{2c_2}{243}P_s^{10} = 0, \quad (4)$$

which obeys the stability conditions

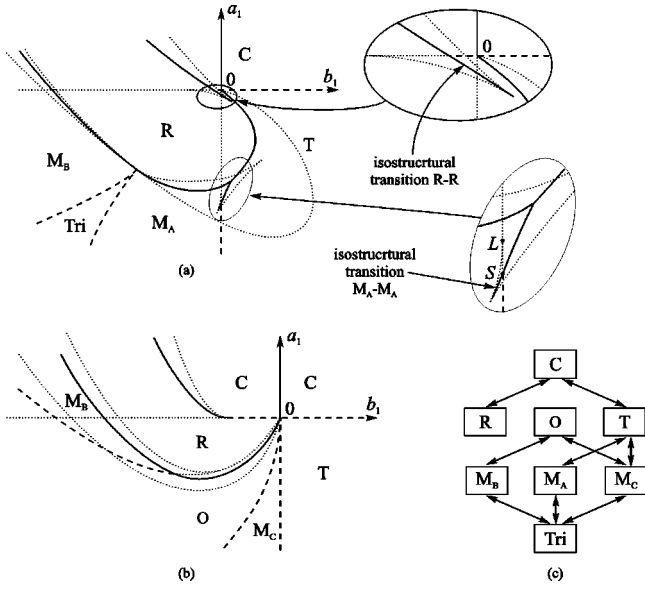


FIG. 1. (a), (b) Phase diagram in  $a_1 b_1$  plane for the potential  $F_{\text{init}}$  for (a)  $c_1 < 0$  and (b)  $c_1 > 0$ . Solid lines are first-order phase boundaries; dashed lines are second-order phase boundaries; dotted lines are stability boundaries of phases. (c) Diagram of possible second-order phase transitions between the phases.

$$(3a_2 + b_1) + \frac{c_1}{3} P_s^2 + 2b_2 P_s^4 + \frac{5c_2}{81} P_s^8 \geq 0, \quad (5)$$

$$b_1 + \frac{c_1}{3} P_s^2 + \frac{2}{3} b_2 P_s^4 + \frac{2c_2}{81} P_s^8 \leq 0. \quad (6)$$

The parametric equations for the boundaries of the phase stability domain are obtained by replacing the inequality in either Eq. (5) or (6) with an equality and solving it together with Eq. (4). The line resulting from Eqs. (4) and (5),

$$a_1(P_s) = \frac{c_1}{9} P_s^4 + \frac{8b_2}{9} P_s^6 + \frac{8c_2}{243} P_s^{10},$$

$$b_1(P_s) = -3a_2 - \frac{c_1}{3} P_s^2 - 2b_2 P_s^4 - \frac{5c_2}{81} P_s^8, \quad (7)$$

has a cusp at  $c_1 < 0$  shown in the top inset of Fig. 1(a). This feature is defined by the parametric equation

$$c_1 + 12b_2 P_{\text{cusp}}^2 + \frac{20c_2}{27} P_{\text{cusp}}^6 = 0. \quad (8)$$

This equation has no real solutions for  $c_1 > 0$ , as the cusp merges with the  $a_1$  axis. Another interesting feature of the phase diagram is a first-order transition line below the  $b_1$  axis, shown in the top inset of Fig. 1(a). It corresponds to an *isostructural* transition between two phases with the same structure and symmetry  $R$ , with the value of  $P_s$  being the only difference between them.<sup>17</sup> Let  $P'_s$  and  $P''_s$  be the two values obtained from the equation of state (4). Then the transition line is defined by  $F_R(P'_s) = F_R(P''_s)$ , where  $F_R(P_s)$  is the potential of phase  $R$ :

$$F_R(P_s) = a_1 P_s^2 + \frac{(3a_2 + b_1)}{3} P_s^4 + \frac{c_1}{27} P_s^6 + \frac{b_2}{9} P_s^8 + \frac{c_2}{729} P_s^{12}. \quad (9)$$

All the equations relating to isostructural phases have an additional permutation symmetry  $P_s'^2 \leftrightarrow P_s''^2$ . Introducing new variables  $U = (P_s'^2 + P_s''^2)/3$  and  $V = P_s'^2 P_s''^2/9$ , which are invariant under the permutation, we obtain

$$6a_1 - c_1(U^2 + 2V) - 18b_2 U^3 - 2c_2 U^3(2U^2 - 5V) = 0,$$

$$a_1 - 4(3a_2 + b_1)U - c_1(2U^2 + V) - 12b_2 U(2U^2 - V) - 2c_2 U^3(2U^2 - 5V) = 0, \quad (10)$$

$$2(3a_2 + b_1) + c_1 U + 12b_2(U^2 - V) + 2c_2(U^4 - 3U^2 V + V^2) = 0.$$

$V$  can be eliminated from Eq. (10) and the resulting equations can be solved for  $a_1$  and  $b_1$ . One of the solutions parametrically defines an isostructural  $R$ - $R$  transition line by

$$a_1(U) = \frac{c_1^2}{18c_2 U} + \frac{b_2 c_1}{c_2} + \frac{c_1}{9} U^2 - 2b_2 U^3 - \frac{4c_2}{9} U^5, \quad (11)$$

$$b_1(U) = -\frac{c_1^2}{36c_2 U^2} - 3a_2 + \frac{9b_2^2}{c_2} - \frac{2c_1}{9} U + 3b_2 U^2 + \frac{5c_2}{9} U^4.$$

A similar isostructural transition line appears in phase  $M_A$  and is shown enlarged in the bottom inset of Fig. 1.

The first-order  $R$ - $C$  transition occurs when the two phases have equal potentials  $F_R(P_s) = 0$ . This condition together with equation of state (4) gives

$$a_1(P_s) = \frac{c_1}{27} P_s^4 + \frac{2b_2}{9} P_s^6 + \frac{4c_2}{729} P_s^{10}, \quad (12)$$

$$b_1(P_s) = -3a_2 - \frac{2c_1}{9} P_s^2 - b_2 P_s^4 - \frac{5c_2}{243} P_s^8.$$

We would like to point out some other important features of the phase diagram of Fig. 1, which can be represented in a simple analytical form. For  $c_1 > 0$ , phase  $M_C$  lies between  $T$ - $M_C$  and  $O$ - $M_C$  second-order phase boundaries defined, respectively, by

$$b_1 = 0 \quad \text{and} \quad b_1 = -\frac{a_1^2 b_2}{8a_2^2}. \quad (13)$$

The second-order  $O$ - $M_B$  transition line is parabolic in the  $(a_1, b_1)$  parameter space

$$(2b_2 a_1 + c_1 b_1)^2 - (c_1^2 + 8a_2 b_2)(c_1 a_1 - 4a_2 b_1) = 0. \quad (14)$$

The lowest-symmetry *Tri* phase appears at  $c_1 < 0$  between phases  $M_A$  and  $M_B$  in a slice restricted by a parametrically defined line

$$\begin{aligned} a_1(t) &= -4a_2t^2 + \frac{c_1a_2}{c_2t^4}, \\ b_1(t) &= -2b_2t^4 + \frac{2c_1b_2}{c_2t^2}, \end{aligned} \quad (15)$$

where  $t$  is a real parameter. The coordinates of the four-phase  $R$ - $M_B$ - $M_A$ -*Tri* critical point can be obtained from Eq. (15):

$$a_1 = 3a_2 \left( \frac{4c_1}{c_2} \right)^{1/3}, \quad b_1 = -3b_2 \left( \frac{2c_1^2}{c_2^2} \right)^{1/3}. \quad (16)$$

The first-order transition lines  $M_B$ - $R$ ,  $R$ - $M_A$ ,  $M_A$ - $T$ , and  $R$ - $O$ , and the isostructural  $M_A$ - $M_A$  line were obtained numerically, as the method described in Eqs. (4)–(12) in these cases leads to high order equations for  $a_1$  and  $b_1$ .

All possible second-order phase transitions are shown in Fig. 1(c). In agreement with the general analysis,<sup>12</sup> only phases  $R$  and  $T$  are accessible from phase  $C$  via a second-order transition. The  $M_C$ -*Tri* second-order transition occurs in the  $c_1 = 0$  plane and is not shown in Fig. 1.

In Sec. III we will give special attention to some other features of the phase diagram shown in the lower inset of Fig. 1(a). They are related to the structure of the phase diagrams, recently observed in PZT (Refs. 3 and 4) and PMN-PT.<sup>5</sup>

### III. PHASE DIAGRAMS OF PZT, PMN-PT, AND PZN-PT

The seemingly simple twelfth-order model potential  $F_{\text{init}}$  from Eq. (3) has led, as can be seen from Fig. 1, to a complex phase diagram describing all eight phases allowed by the symmetry of the problem. All possible second-order phase transitions among the proper ferroelectric phases in perovskites are established by Fig. 1(c), so any approximations made to describe transitions driven by the ferroelectric order parameter should not add or forbid any second-order transition lines obtained in the model [Eq. (3)]. On the other hand, first-order phase transitions between any two of the eight phases can be expected, since, in general, there are no arguments that can forbid these transitions. For example, a direct  $O$ - $T$  transition has been experimentally observed in PZN-PT (Ref. 7) and earlier in BaTiO<sub>3</sub>.

In Fig. 2 we plot the experimental phase diagrams of PZT and PZN-PT together with our calculations based on the model described. In Sec. II we have shown that the triple point of phases  $R$ ,  $T$ , and  $M_A$  can appear as an intersection of the first-order phase transition lines [see Fig. 1(a)]. A second-order phase transition  $M_A$ - $T$  is possible below the critical point  $S$ . This is exactly the topological structure of the  $M_A$ - $T$  phase transition line that has been observed in PZT.<sup>3</sup> To obtain reasonable agreement with the experiment, we assumed that the coefficients  $a_1$  and  $b_1$  in Eq. (3) are linear functions

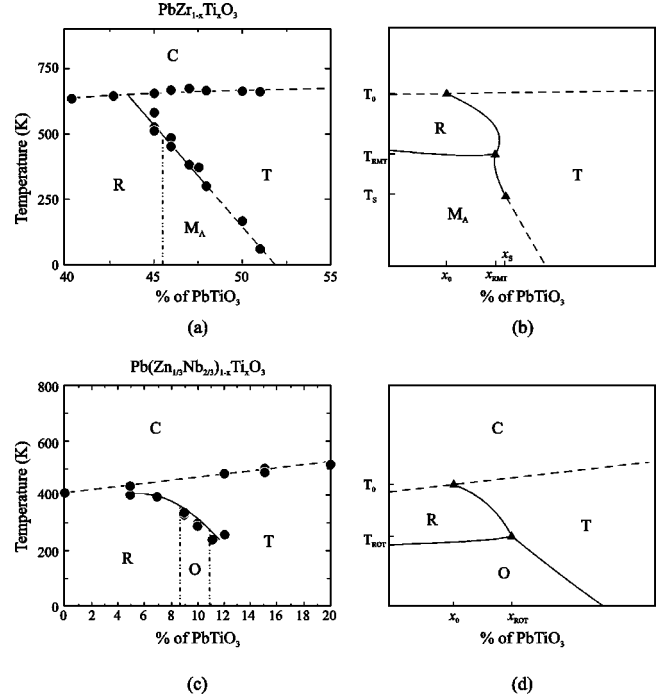


FIG. 2. (a), (c) Phase diagrams of PZT and PZN-PT from Refs. 3,4,6 and 18. (b), (d) Phase diagrams calculated based on the model potentials  $F_{\text{PZT}}$  and  $F_{\text{PZN}}$ , as described in the text. Critical points are shown as triangles, their coordinates are marked on axes.

of temperature and composition, while the rest of the parameters are constant:

$$\begin{aligned} a_1 &= \alpha_T(T - T_0) + \alpha_x(x - x_0), \\ b_1 &= \beta_T(T - T_0) + \beta_x(x - x_0). \end{aligned} \quad (17)$$

Keeping in mind the global topology of the phase diagram shown in Fig. 1, we can identify the features related to the piezoelectric compounds. When applying the developed model to the particular systems, we add some symmetry-allowed terms to the expansion [Eq. (3)]. This enables us to use simple temperature and concentration dependencies of the phenomenological parameters while achieving a good fit to the experimental phase diagrams. To model a PZT-type phase diagram (also related to PMN-PT), we use an expansion for the Landau potential

$$F_{\text{PZT}} = F_{\text{init}} + d_{12}J_1J_2. \quad (18)$$

Upon this modification, the  $M_A$ - $T$  second-order transition line remains straight but becomes tilted with respect to the  $a_1$  axis:

$$b_1 = \frac{d_{12}a_1}{2a_2}. \quad (19)$$

Since the phenomenological phase diagram can always be isomorphically transformed to fit the experimental data, we do not try to obtain a perfect quantitative fit. Rather, we

TABLE I. Parameters of the Landau potentials used for qualitative fit of phase diagrams for PZT and PZN- $x$ PT.

Parameter	Value for $F_{\text{PZT}}$	Value for $F_{\text{PZN}}$
$\alpha_T$	1	1
$\alpha_x$	-0.07	-0.8
$\beta_T$	0.05	0.6
$\beta_x$	1	1
$c_1$	-25	-40
$a_2$	9	9
$b_2$	0.8	0.7
$c_2$	3.6	0
$d_{12}$	-0.3	8
$d_{13}$	0	13

calculate the coefficients in arbitrary units to reproduce the qualitative features of the phase diagrams. The calculated values are shown in Table I.

We used a relatively large absolute value for  $c_1$  to obtain comparable lengths of the first-order  $M_A$ - $T$  transition line and  $R$ - $T$  phase boundary, modeling the experimental data for PZT. This results in a vanishingly small region of coexistence of the two isostructural  $M_A$  phases [see the bottom inset in Fig. 1(a)]. The critical point  $S$  then almost merges with point  $L$ , the latter being a tangency point of the  $T$ - $M_A$  second-order transition line continuation and the stability boundary of phase  $M_A$ .

For the expansion (18), point  $L$  has these coordinates:

$$a_1 = \frac{2a_2^2 c_1}{4a_2 b_2 - d_{12}^2}, \quad b_1 = \frac{a_2 c_1 d_{12}}{4a_2 b_2 - d_{12}^2}. \quad (20)$$

More extensive modifications of  $F_{\text{init}}$  have been used to accommodate the features of the experimental phase diagram of PZN-PT, namely a direct  $O$ - $T$  transition and, more importantly, the separation of the triple points  $R$ - $O$ - $T$  and  $C$ - $R$ - $T$ :

$$F_{\text{PZN}} = F_{\text{init}} + d_{12} J_1 J_2 + d_{13} J_1 J_3. \quad (21)$$

We find that the part of the global phase diagram, relevant to PZN-PT, is almost unaffected by the variation of  $c_2$ . Therefore, we assume  $c_2 = 0$ . The other coefficients are found in Table I.

#### IV. PIEZOELECTRIC PROPERTIES

Elastic energy and electrostrictive coupling have to be introduced into Landau potential to obtain the components of the piezoelectric tensor  $d_{ik}$ . The piezoelectric constants are inversely proportional to combinations of the second derivatives of  $F_{\text{PZT}}$  and  $F_{\text{PZN}}$  with respect to  $P_x, P_y, P_z$ .<sup>19</sup> Some of these combinations vanish at the stability boundaries of the phases, resulting in anomalous values of the piezoelectric constants.

By analyzing the phase stability conditions obtained in Sec. II, we find the components  $d_{ik}$ , which can be large for each phase of the phase diagrams in Fig. 2. In the  $R$  phase,

all four independent piezoelectric constants are expected to be large at all the phase transition lines with phases  $T$ ,  $M_A$ , and  $O$ .

The tetragonal piezoelectric  $d_{15}$  (in this section we use a pseudocubic orthogonal basis in the  $d_{ik}$  notation) component of the piezoelectric tensor can be large at the  $T$ - $R$ ,  $T$ - $M_A$ , and  $T$ - $O$  phase boundaries, while  $d_{33}$  and  $d_{31}$  are not expected to have anomalies in temperature and composition dependence at these lines.

A complex behavior of the piezoelectric constants is expected in phase  $M_A$  at the boundary with phase  $T$ . In the second-order transition part of this phase boundary, no anomalies are expected. This is because no stability condition is violated there, even though it is a bifurcation line where the monoclinic solution of the equations of state becomes imaginary. However, this situation changes drastically when  $M_A$ - $T$  is a first-order phase transition. In this part of the  $M_A$ - $T$  boundary and at the  $M_A$ - $R$  boundary, all ten monoclinic piezoelectric coefficients can be large.

Another verifiable prediction of our theory is the connection between the proximity of phase  $M_A$  to the triclinic distortion and anomalies in the monoclinic piezoelectric coefficients  $d_{11}$ ,  $d_{12}$ ,  $d_{14}$ , and  $d_{15}$ , at low temperatures. Finally,  $d_{33}$  and  $d_{31}$  can be large in phase  $O$  at the  $T$  boundary and also  $d_{24}$  at the  $R$  boundary.

#### V. SUMMARY AND DISCUSSION

We have shown that the increasingly high-order phenomenological models, used to describe the highly nonlinear piezoelectric systems PZT, PMN-PT, and PZN-PT, are approximations of a complete twelfth-order model (2). Such a complex model is difficult to analyze, but even the significantly simplified model potentials  $F_{\text{PZT}}$  and  $F_{\text{PZN}}$  describe the phase diagram of the compounds reasonably well, as seen in Fig. 2. We have allowed for some discrepancy between the calculated and the experimental phase diagrams, for example, in the location of  $R$ - $M_A$  and  $R$ - $O$  phase boundaries, in order to keep the dependence of the phenomenological parameters on temperature and concentration as simple as possible. On the other hand, it is clear that since our phenomenological models correctly describe the qualitative features of the phase diagram, a complete quantitative agreement can be achieved by a careful fitting of the phenomenological parameters to the experimental data.

The important features that our simple models correctly reproduce are the separation of the triple points  $R$ - $O$ - $T$  and  $R$ - $M_A$ - $T$  from the  $C$ - $R$ - $T$  triple point, and the switching of the  $M_A$ - $T$  phase transition between the first- and the second-order types.

We also predict an anomalous behavior of certain piezoelectric constants along the phase transition lines. These predictions elucidate the nature of the ultrahigh piezoelectricity and make our theory easily verifiable. To our knowledge, systematic measurements of evolution of the piezoelectric constants in the vicinity of the newly found phase boundaries in PZT, PMN-PT, and PZN-PT have not been done yet.

Finally, group-theoretical and catastrophe-theory methods of phase transition theory described in this paper stand on

their own. We described a general approach that puts phenomenological analysis on firm footing, and minimizes the necessary amount of numerical calculations.

### ACKNOWLEDGMENTS

We would like to thank M. F. Kurpriyanov, E. S. Larin, D. Vanderbilt, and G. Gaeta for very helpful comments and discussions.

### APPENDIX A: CALCULATION OF IRBI FOR REPRESENTATIONS OF SPACE GROUPS

Let  $\mathcal{L}$  be the group of all different matrices of a  $p$ -dimensional representation of a space group. The  $\mathcal{L}$  group can be thought of as a point group in the space of the order parameter components  $\eta_i$ ,  $i = 1, \dots, p$ . The Landau potential is invariant under transformations of this group.

The integrity rational basis of invariants (IRBI) of the  $\mathcal{L}$  group is a minimal set of homogeneous  $\mathcal{L}$ -invariant polynomials depending on  $\eta_i$  such that any other invariant homogeneous polynomial is an algebraic combination of the elements of this set. One of the methods to find the IRBI is described briefly below.<sup>11</sup>

It can be proved that for every group  $\mathcal{L}$  the following sequence of subgroups can be constructed:

$$E \equiv \mathcal{L}_0 \subset \mathcal{L}_1 \subset \dots \subset \mathcal{L}_N \equiv \mathcal{L}, \quad (\text{A1})$$

where each  $\mathcal{L}_i$  is an invariant subgroup of  $\mathcal{L}_{i+1}$  and  $E$  the identity group.

The problem of constructing IRBI of  $\mathcal{L}$  is reduced to constructing invariants of the factor groups

$$\mathcal{A}_i = \mathcal{L}_i / \mathcal{L}_{i-1} \quad (\text{A2})$$

at every step of Eq. (A1). It turns out that for any  $\mathcal{L}$  group,  $\mathcal{A}_i$  acts on the invariants obtained in the previous  $(i-1)$ th step as cyclic group of order 2 or 3, for which the invariants can be easily constructed. Removing the algebraic dependencies among the polynomials thus obtained at each step, at the  $N$ th step one obtains the IRBI for the given  $\mathcal{L}$  group.

If  $m$  is the number of invariants constituting the IRBI for a space group representation, then, in general,  $m \geq p$ , and there exist  $m-p$  algebraic relations of higher than first order among the  $m$  invariant polynomials. However, for irreducible representations of groups generated by reflections  $m=p$ . This is the situation for the ferroelectric order parameter in  $Pm3m$  group, for which the step-by-step calculation of invariants results in the IRBI [Eq. (1)]. The method described here allows for a simple generalization to groups with continuous subgroups, such as a gauge transformation group.<sup>11,20</sup>

### APPENDIX B: STRUCTURAL STABILITY OF PHENOMENOLOGICAL POTENTIALS

In this appendix we review the method based on catastrophe theory, which is used to analyze the stability of the potential functions. We consider the simplest case of an irreducible representation of a group generated by reflections, for which  $m=p$  (see Appendix A).

To determine the structural stability of some potential function  $F(J_1, \dots, J_m)$ , we need to introduce the algebraic combinations:

$$U_i(J_1, \dots, J_m) = \sum_{k=1}^m \frac{\partial F}{\partial J_k} (\nabla J_k, \nabla J_i), \quad i = 1, \dots, m \quad (\text{B1})$$

where  $\nabla J_i$  is the gradient of invariant  $J_i$  in the order parameter space. Scalar products that appear in Eq. (B1) can always be expressed in terms of invariant polynomials  $J_1, \dots, J_m$ . A term can be omitted in the potential function without violating the type of the extremal behavior of this function if its coefficient is small and if it can be expressed as

$$\sum_{i=1}^m \mathcal{P}_i(J_1, \dots, J_m) U_i(J_1, \dots, J_m) + (\text{higher-order terms}). \quad (\text{B2})$$

Here  $\mathcal{P}_i(J_1, \dots, J_m)$  are some polynomials.

Following this algorithm, we obtain for the integrity basis (1) and potential (3)

$$(\nabla J_1)^2 = 4J_1, \quad (\nabla J_1, \nabla J_2) = 8J_2,$$

$$(\nabla J_2)^2 = 4J_1J_2 + 12J_3, \quad (\nabla J_2, \nabla J_3) = 8J_1J_3, \quad (\text{B3})$$

$$(\nabla J_3)^2 = 4J_2J_3, \quad (\nabla J_1, \nabla J_3) = 12J_3.$$

and

$$U_1 = 4a_1J_1 + (\text{higher-order terms}),$$

$$U_2 = 8a_1J_2 + (\text{higher-order terms}), \quad (\text{B4})$$

$$U_3 = 12a_1J_3 + (\text{higher-order terms}).$$

It is now clear that every term in Eq. (2), additional to Eq. (3), can be represented in the form (B2). However, there is another restriction that arises from the requirement for a model to produce all the phases allowed by the symmetry of the order parameter. As can be seen from Eq. (15), the triclinic phase cannot appear in the phase diagram of the truncated below the twelfth-order Landau potential expansion (3). Consequently, the potential (3) is the simplest model that meets all the requirements mentioned above.

\*Email address: iserg@uic.rsu.ru

- <sup>1</sup>B. Noheda, J. A. Gonzalo, A. C. Caballero, C. Moure, D. E. Cox, and G. Shirane, *Appl. Phys. Lett.* **74**, 2059 (1999).
- <sup>2</sup>B. Noheda, J. A. Gonzalo, L. E. Cross, R. Guo, S.-E. Park, D. E. Cox, and G. Shirane, *Phys. Rev. B* **61**, 8687 (2000).
- <sup>3</sup>B. Noheda, D. E. Cox, G. Shirane, R. Guo, B. Jones, and L. E. Cross, *Phys. Rev. B* **63**, 014103 (2001).
- <sup>4</sup>D. La-Orautapong, B. Noheda, Z.-G. Ye, P. M. Gehring, J. Toulouse, D. E. Cox, and G. Shirane (unpublished); cond-mat/0108264 (unpublished).
- <sup>5</sup>Z.-G. Ye, B. Noheda, M. Dong, D. Cox, and G. Shirane, *Phys. Rev. B* **64**, 184114 (2001).
- <sup>6</sup>B. Jaffe, W. R. Cook, and H. Jaffe, *Piezoelectric Ceramics* (Academic Press, London, 1971).
- <sup>7</sup>B. Noheda, D. E. Cox, G. Shirane, S.-E. Park, L. E. Cross, and Z. Zhong, *Phys. Rev. Lett.* **86**, 3891 (2001).
- <sup>8</sup>A. F. Devonshire, *Philos. Mag.* **40**, 1040 (1949); **42**, 1065 (1951); *Adv. Phys.* **3**, 85 (1954).
- <sup>9</sup>I. S. Zheludev and L. A. Shuvalov, *Kristallografiya* **1**, 681 (1956).
- <sup>10</sup>Yu. M. Gufan, *Fiz. Tverd. Tela* **13**, 225 (1971) [*Sov. Phys. Solid State* **13**, 175 (1971)].
- <sup>11</sup>Yu. M. Gufan, *Structural Phase Transitions* [in Russian] (Nauka, Moscow, 1982).
- <sup>12</sup>Yu. M. Gufan and V. P. Sakhnenko, *Zh. Éksp. Teor. Fiz.* **69**, 1429 (1975) [*Sov. Phys. JETP* **42**, 728 (1975)].
- <sup>13</sup>L. Bellaiche, A. Garcia, and D. Vanderbilt, *Phys. Rev. Lett.* **84**, 5427 (2000).
- <sup>14</sup>D. Vanderbilt and M. H. Cohen, *Phys. Rev. B* **63**, 094108 (2001).
- <sup>15</sup>A. M. Prokhorov, Yu. M. Gufan, E. S. Larin, E. G. Rudashevski, and V. B. Shirokov, *Dokl. Akad. Nauk SSSR* **277**, 1369 (1984) [*Sov. Phys. Dokl.* **29**, 656 (1984)].
- <sup>16</sup>V. I. Arnold, A. N. Varchenko, and S. M. Gusein-Zade, *Singularities of Differentiable Maps. The Classification of Critical Points, Caustics and Wave Fronts*, edited by V. I. Arnold (Birkhäuser, Boston, 1985); R. Gilmore, *Catastrophe Theory for Scientists and Engineers* (Wiley, New York, 1981).
- <sup>17</sup>Yu. M. Gufan and E. S. Larin, *Dokl. Akad. Nauk SSSR* **242**, 1311 (1978) [*Sov. Phys. Dokl.* **23**, 754 (1978)].
- <sup>18</sup>J. Kuwata, K. Uchino, and S. Nomura, *Ferroelectrics* **37**, 579 (1981).
- <sup>19</sup>M. J. Haun, E. Furman, S. J. Jang, and L. E. Cross, *Ferroelectrics* **99**, 13 (1989).
- <sup>20</sup>Yu. M. Gufan, *Zh. Éksp. Teor. Fiz.* **107**, 855 (1995) [*Sov. Phys. JETP* **80**, 485 (1995)].